Self-Mixing Interferometric Sensor Displacement Reference for PPG Motion Artifact Handling

Ralph W.C.G.R. Wijshoff,
Ronald M. Aarts
Eindhoven University of Technology
Department of Electrical Engineering
Signal Processing Systems Group
Eindhoven, The Netherlands
Email: r.w.c.g.r.wijshoff@tue.nl,
r.m.aarts@tue.nl

Jeroen Veen,
Alexander M. van der Lee
Philips Research
Biomedical Sensor Systems Group
and Light Generation Group
Eindhoven, The Netherlands
Email: jeroen.veen@philips.com,
alexander.van.der.lee@philips.com

Cristian Presura
Philips Applied Technologies
Systems in Package Group
Eindhoven, The Netherlands
Email: cristian.presura@philips.com

***Abstract*—By illuminating the skin, a photoplethysmograph can measure a patient's heart rate and blood oxygenation. The optical signals measured (PPGs) are highly susceptible to motion, which can distort the PPG derived data. It is hypothesized that motion induced optical artifacts in PPGs correlate to movement of the sensor with respect to the skin. To investigate this correlation, a displacement measuring method using the self-mixing interferometric effect of a laser diode has been designed and tested in a laboratory setup. It is shown that displacement between the laser diode and a skin phantom can be measured accurately using the proposed method. Therefore the proposed method can be applied to measure displacement between a PPG sensor and skin and used to determine whether sensor displacement correlates to optical motion artifacts in PPGs.**

***Index Terms*—motion artifacts, photoplethysmography, self-mixing interferometry**

I. Introduction

Currently, photoplethysmography is widely applied in operating rooms and intensive care units to measure a patient's heart rate and blood oxygenation. It is foreseen that this technology will be applied in ambulatory settings in the near future, such as general wards and the patients' homes [1]. To reliably measure PPGs in ambulant patients, motion robustness of photoplethysmographs needs to be improved significantly. An important class of PPG motion artifacts is caused by changing optical coupling and tissue compression as a result of movement of the sensor with respect to the skin. This research aims at removing these optical motion artifacts from PPGs.

In this research it is hypothesized that the optical motion artifacts in a PPG correlate to movement of the sensor with respect to the skin. In this case, the optical motion artifacts can be detected or corrected using a measure of sensor displacement, which is considered to outperform (non-linear) PPG post-processing methods not employing a measured motion reference [2]. As a first step to test this hypothesis, sensor displacement has been measured in a laboratory setup using self-mixing interferometry (SMI). SMI is measured by a laser diode's internal photodiode, and therefore is a self-aligning, compact and cheap solution which can be integrated in a PPG sensor. Moreover, this method assures measuring motion of the light source itself, rather than measuring offset sensor motion using accelerometers or additional optical sensors [1], [2].

In Section II it is explained how sensor displacement can be measured via an SMI method that requires amplitude modulation of the laser current. This method has been tested in a laboratory setup. Here the laser diode illuminates a diffuse scattering Delrin skin phantom mounted on a loudspeaker, to mimic sensor motion with respect to the skin. Results thus obtained are presented and discussed in Sections III and IV respectively. The experimental results demonstrate that sensor displacement with respect to a skin phantom can be measured accurately via SMI using the proposed method.

II. SMI Theory

SMI is observed when a laser diode illuminates an external target such that part of the light backscattered by the target enters the laser diode's cavity again (Fig. 1). The backscattered light interferes with the standing wave pattern inside the laser cavity, thus changing the emitted optical lasing frequency and power [4]. Movement of the external target by half of the emitted wavelength thus results in a full cycle in emitted

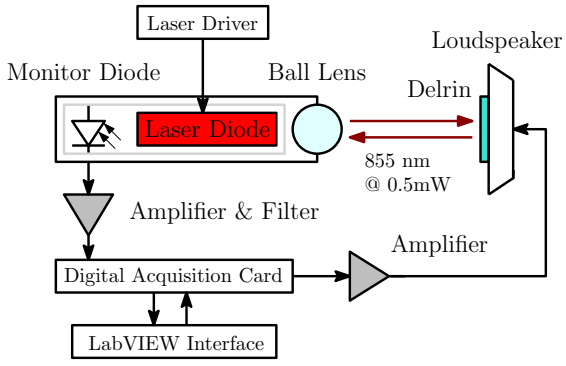

Figure 1. Schematic of the experimental setup built to measure sensor motion with respect to a Delrin skin phantom. Via a ball lens the laser light is focussed onto a piece of Delrin, which is attached to a loudspeaker. A laser driver amplitude modulates the laser current to induce a continuous wavelength modulation. A LabVIEW interface controls a data acquisition card to record the amplified and filtered monitor diode current and to steer the loudspeaker.

optical power. The target's displacement then follows by counting the number of cycles in the emitted optical power.

However, only counting the number of cycles in the optical power does not reveal the direction of motion. Without directional information the displacement measurement may have a frequency twice as high as the displacement itself, complicating its use to correct motion artifacts in PPGs. Using SMI, the direction of motion can be obtained from the shape of the interference pattern in the optical power or by emitting multiple wavelengths. At high levels of optical feedback the interference pattern is sawtooth shaped, of which the direction of the fast edge depends on the direction of motion [3]. Such high levels of optical feedback may not be obtained because of the diffuse optical scattering of skin though. Therefore an amplitude modulation of the laser current is applied which induces a continuous wavelength modulation. In this case the direction of motion can be recovered by using the phase relationship between the different wavelengths emitted.

The fluctuations in optical power over time t [s] as a result of target motion can be measured by the laser diode's internal monitor diode. The monitor diode's current is proportional to the SMI effect and is therefore considered to be the SMI signal. The monitor diode's current can be expressed as:

$$i_{MD}(t) = \frac{\eta q}{h\nu}\left(P_{DC} + \Delta P_m(t) + \Delta P_{fb}(t)\right), \quad (1)$$

in which η [-] is the monitor diode's efficiency, q [C] the electron charge, h [Js] Planck's constant, ν [Hz] the optical frequency emitted, P_{DC} [W] the DC optical power in the laser cavity, and $\Delta P_m(t)$ [W] and $\Delta P_{fb}(t)$ [W] the fluctuations in optical power caused by modulation and optical feedback respectively. The target's displacement information is contained in the latter term, for which it holds that [3]:

$$\Delta P_{fb}(t) \sim \cos\left(2\pi\nu\tau_{ext}\right), \quad (2)$$

in which $\tau_{ext} = 2L_{ext}/c$ [s] is the round trip time in the external cavity of length L_{ext} [m] between laser diode and target, with c [m/s] the speed of light. This relationship shows that the optical power in the cavity increases maximally when the backscattered light is in phase and decreases maximally when the backscattered light is in antiphase. To determine the influence of modulation and target motion on this term, it is assumed that amplitude modulation of the laser current at ω_m [rad/s] with initial phase ϕ_m [rad] yields a time-varying emitted wavelength $\lambda(t) = \lambda_0 + \Delta\lambda_m \sin(\omega_m t + \phi_m)$ [m], that the mean distance between laser diode and target L_0 [m] changes over time by $\Delta L(t)$ [m] and that optical feedback yields a wavelength change of $\Delta\lambda_{fb}(t)$ [m]. As these fluctuations are small compared to the mean values, Eq. (2) can be approximated by:

$$\begin{aligned}\Delta P_{fb}(t) \approx \cos\Bigg[&4\pi\frac{L_0}{\lambda_0}\left(1 + \frac{\Delta L(t)}{L_0} - \frac{\Delta\lambda_{fb}(t)}{\lambda_0}\right)\\ &- \frac{\phi_0}{2}\left(1 + \frac{\Delta L(t)}{L_0}\right)\sin(\omega_m t + \phi_m)\Bigg], \quad (3)\end{aligned}$$

in which ϕ_0 is the approximate difference in phase between the backscattered light with the longest and shortest wavelengths at mean distance L_0:

$$\frac{4\pi L_0}{\lambda_0 - \Delta\lambda_m} = \frac{4\pi L_0}{\lambda_0 + \Delta\lambda_m} + \phi_0 \rightarrow \phi_0 \approx 8\pi L_0 \frac{\Delta\lambda_m}{\lambda_0^2}. \quad (4)$$

Via the Jacobi-Anger expansion Eq. (3) can be expanded into signals in baseband, around the modulation frequency and around the second harmonic of the modulation frequency:

$$\begin{aligned}\Delta P_{fb}(t) \approx 2J_1\left(\phi_0(t)\right)\sin\left(\omega_m t + \phi_m\right)\sin\left(\phi_t(t)\right) +\\ \left[J_0\left(\phi_0(t)\right) + 2J_2\left(\phi_0(t)\right)\cos\left(2(\omega_m t + \phi_m)\right)\right]\cos\left(\phi_t(t)\right), \quad (5)\end{aligned}$$

in which J_n is the n^{th} Bessel function of the first kind, and:

$$\phi_0(t) = \frac{\phi_0}{2}\left(1 + \frac{\Delta L(t)}{L_0}\right), \quad (6)$$

$$\phi_t(t) = \frac{4\pi}{\lambda_0}\left(L_0 + \Delta L(t)\right) - \frac{4\pi L_0}{\lambda_0^2}\Delta\lambda_{fb}(t), \quad (7)$$

$$\Delta L(t) = \int_0^t v(\xi)d\xi = \frac{\lambda_0}{2}\int_0^t f_d(\xi)d\xi, \quad (8)$$

with $v(t)$ [m/s] the target's velocity and $f_d(t)$ [Hz] the Doppler frequency caused by motion. The expansion in Eq. (5) shows that the light backscattered into the laser cavity by the moving target yields Doppler signals with a phase $\phi_t(t)$ as in Eq. (7). The target's displacement $\Delta L(t)$ appears both in $\phi_0(t)$ and $\phi_t(t)$. Displacement $\Delta L(t)$ is reconstructed using $\phi_t(t)$, because uncertainties and perturbations in the amplitude of $i_{MD}(t)$ complicate recovering $\phi_0(t)$. As modulation causes $\phi_t(t)$ to appear both in a sine and a cosine, it can be recovered conveniently by tracking the phase of the rotating vector of which the sine and cosine terms are the Cartesian coordinates. Moreover, Eq. (5) shows that $\cos(\phi_t(t))$ appears both in the baseband and around the second harmonic. The $\cos(\phi_t(t))$ term around the second harmonic will be used for the displacement measurements, because it has a better SNR given the $1/f$ noise characteristic and mains interference.

The vertical coordinate of the rotating vector is obtained by demodulating the SMI signal with the modulation frequency, and passing the result through a low-pass filter (LPF) with a cut-off at the maximum Doppler frequency $\omega_{d\,\max} < \omega_m$:

$$i_y(t) = 2 \cdot \text{LPF}\left\{i_{MD}(t) \cdot \sin\left(\omega_m t + \phi_m\right)\right\} \quad (9)$$

$$\sim A_{1st} + 2J_1\left(\phi_0(t)\right)\sin\left(\phi_t(t)\right), \quad (10)$$

in which A_{1st} [-] results from the amplitude modulation of the laser current. The horizontal coordinate of the rotating vector is obtained similarly by demodulating the SMI signal with double the modulation frequency, and passing the result through the same low-pass filter:

$$i_x(t) = 2 \cdot \text{LPF}\left\{i_{MD}(t) \cdot \cos\left(2(\omega_m t + \phi_m)\right)\right\} \quad (11)$$

$$\sim A_{2nd} + 2J_2\left(\phi_0(t)\right)\cos\left(\phi_t(t)\right), \quad (12)$$

in which A_{2nd} [-] is proportional to the second harmonic of the modulation frequency in the SMI signal. Target displacement now can be reconstructed by tracking the phase of the rotating vector $(i_x(t), i_y(t))$ and equating each full rotation of 2π rad to a displacement of half a wavelength. In practice however, Eqs. (10) and (12) are perturbed by additive noise terms $n_x(t)$

and $n_y(t)$ respectively, caused by shot noise, thermal noise and quantization noise. These noise terms influence the accuracy of the method. Taking into account these noise sources, the displacement reconstruction method can be expressed as:

$$\Delta L_{smi}(t) = \frac{\lambda_0}{4\pi}\text{unwrap}\left[\arctan\left(\frac{y_n(t)+n_{yn}(t)}{x_n(t)+n_{xn}(t)}\right)\right] \quad (13)$$

$$\approx L_0 + \Delta L(t) - \frac{L_0}{\lambda_0}\Delta\lambda_{fb}(t) + \frac{\frac{\lambda_0}{4\pi}\tan(\phi_t(t))}{1+\tan^2(\phi_t(t))}\cdot \left[\left(\frac{A_y(t)}{A_x(t)}-1\right) + \frac{\frac{n_{yn}(t)}{\tan(\phi_t(t))} - n_{xn}(t)}{A_x(t)\cos(\phi_t(t))}\right] \quad (14)$$

$$\leq L_0 + \Delta L(t) + \frac{\lambda_0}{4\pi}C + \frac{\lambda_0}{8\pi}\cdot \max_t\left[\left(\frac{A_y(t)}{A_x(t)}-1\right) + \frac{n_{xn}(t)+n_{yn}(t)}{A_x(t)/2}\right], \quad (15)$$

in which $x_n(t), y_n(t)$ are the normalized, zero mean versions of $i_x(t), i_y(t)$ respectively, $n_{xn}(t), n_{yn}(t)$ are the normalized noise terms, $A_x(t) \approx 1, A_y(t) \approx 1$ are the amplitudes of the normalized coordinates, and the change in wavelength as a result of optical feedback has been upper bounded using the lasing condition and optical feedback parameter C [-] as explained in [4]. Equation (15) shows the upper bound of three additive noise sources which distort the displacement reconstruction. The first noise source is caused by the change in emitted optical wavelength as a result of optical feedback and has been upper bounded by $(\lambda_0 C)/(4\pi)$. Since only weak feedback regimes are expected in this application, it holds that the feedback parameter $C < 1$ [4]. Therefore this error term will have a magnitude in the order of $(\lambda_0 C)/(4\pi) \approx 10^{-8}$ m. The second noise source is caused by imperfect normalization as a result of which $A_x(t) \approx A_y(t)$. Assuming that normalization is effective such that $\max_t(A_y(t)/A_x(t)) \approx 1$, this error will have a magnitude in the order of 10^{-8} m as well. Finally, since the Doppler frequencies centered at the modulation frequency and second harmonic are used, it is expected that $2\max_t((n_{xn}(t)+n_{yn}(t))/A_x(t))$ is smaller than one as well, yielding an error of 10^{-8} m as a result of shot noise, thermal noise and quantization noise. Since sensor displacement is expected to be in the order of $10^{-4} - 10^{-3}$ m, these error sources introduce an error of roughly 0.1‰.

III. Experimental Results

The experimental setup in Fig. 1 has been built to verify the theory presented in the previous section. To simulate displacement between sensor and skin, a diffuse scattering Delrin skin phantom is attached to a loudspeaker that moves sinusoidally at 3 Hz. A ball lens focusses the laser beam of an 855 nm VCSEL (Vertical-Cavity Surface-Emitting Laser Diode) onto the Delrin. The mean distance between laser diode and Delrin is $L_0 \approx 1$ cm. The emitted optical power is 0.5 mW, obtained by a 2.1 mA DC driving current. An AC component at 40 kHz with an amplitude of 41 μA is superimposed onto the DC current, to introduce a phase shift $\phi_0(t)$ that assures a large amplitude of $i_x(t), i_y(t)$ and sufficient distance

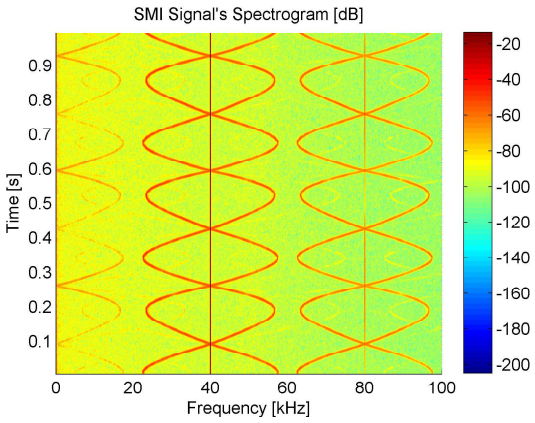

Figure 2. Spectrogram of the monitor diode current. The amplitude modulation yields a frequency component at 40 kHz. The loudspeaker moving at 3 Hz causes Doppler frequencies which vary sinusoidally over time.

from the zero crossings of $J_1(\phi_0(t)), J_2(\phi_0(t))$ (Eq. (5)). This situation can be conveniently recognized by the disappearing baseband signal, because $J_1(\phi_0(t)), J_2(\phi_0(t))$ approach their maximum when $J_0(\phi_0(t)) \approx 0$. The monitor diode current is digitized by a 16 bit digital acquisition card at 200 kHz, after being band limited at 100 kHz. To determine the accuracy of the SMI displacement measurement, it has been compared to a displacement measurement obtained by a Laser Distance Triangulation Sensor with a resolution of 4.5 μm.

Figure 2 shows the spectrogram of the monitor diode current, measured when the laser diode illuminates the Delrin skin phantom moving at 3 Hz. The moving Delrin causes Doppler frequencies that vary sinusoidally over time, as can be observed in baseband, around the modulation frequency at 40 kHz and its second harmonic at 80 kHz. The Doppler signals in baseband are weaker than the Doppler signals at 40 kHz and 80 kHz because of the modulation depth used. Figure 2 also illustrates the higher noise level in the baseband.

The Cartesian coordinates of the rotating vector are obtained from the SMI signal by demodulation as described by Eqs. (9) and (11). The carriers required for demodulation are conveniently obtained by band pass filtering the SMI signal at 40 kHz and the SMI signal squared at 80 kHz. Examples of the resulting normalized, zero mean coordinates $x_n(t), y_n(t)$ are respectively shown in solid blue and dashed red in Fig. 3a. Normalization is achieved by dividing $i_x(t), i_y(t)$ by their 500 Hz low-pass filtered square multiplied by two. In the fragment in Fig. 3a, the loudspeaker reverses direction between 0.424 s and 0.426 s, as indicated by the constant values of the coordinates in this interval. One can observe that the direction of motion is conveyed by the order of the local extremes in $x_n(t)$ and $y_n(t)$, since this order changes before and after this interval. The order of the local extremes determines the vector's direction of rotation. Figure 3a also shows the increasing Doppler frequency as a result of the loudspeaker's increasing speed of motion. Moreover, for this measurement it holds that $A_y(t)/A_x(t) = 1.00 \pm 0.131$ indicating that imperfections in normalization result in an error in the order

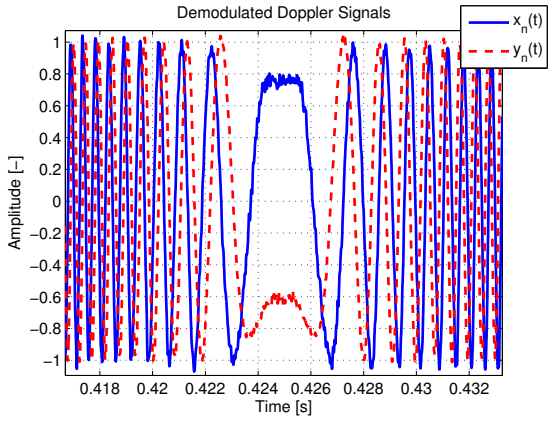

(a) Normalized, zero mean vector coordinates $(x_n(t), y_n(t))$.

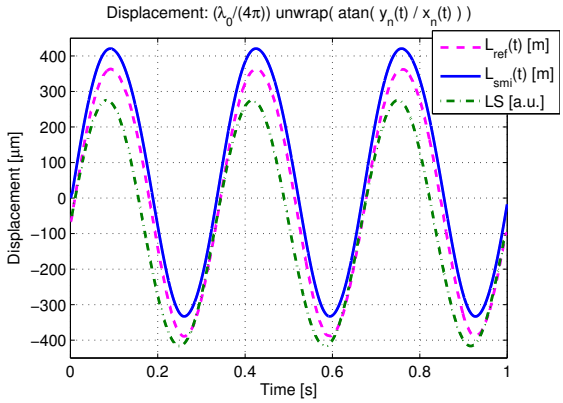

(b) Displacement from SMI $(L_{smi}(t))$ and reference $(L_{ref}(t))$, and the scaled loudspeaker control voltage (LS).

Figure 3. Results obtained for a loudspeaker moving at 3 Hz. The order of the local extremes in $(x_n(t), y_n(t))$ conveys the direction of motion, as shown in Fig. 3a. The equality in shape of the SMI and reference displacement measurements is illustrated in Fig. 3b, as well as the equality of the time delays between the displacements and the loudspeaker's control voltage.

of 10^{-8} m, assuming a maximum of three times the standard deviation (Eq. (15)). A background measurement without target illumination has shown that the normalized noise terms $n_{xn}(t), n_{yn}(t)$ respectively equal 0.041 and 0.037 RMS, and that $2(n_{xn}(t) + n_{yn}(t))/A_x(t) = 0.111$ RMS. Assuming a maximum of three times the standard deviation, it follows that shot noise, thermal noise and quantization noise result in a displacement error in the order of 10^{-8} m (Eq. (15)).

Figure 3b shows the reconstructed displacement obtained via Eq. (13) in solid blue, the reference displacement measurement in dashed magenta and the scaled loudspeaker control voltage in dash-dotted green. The full displacement measured via SMI equals 754 ± 0.199 μm, and the reference yields a full displacement of 751 ± 1.94 μm. Both displacement measurements show a lag with respect to the control voltage. The SMI method yields a lag of 9.67 ± 1.34 ms, and the reference yields a lag of 10.1 ± 1.68 ms.

IV. Discussion

The experiments show that displacement of a diffuse scattering Delrin skin phantom can be accurately reconstructed using SMI, applying the theory outlined in Section II. Demodulation as described by Eqs. (9) and (11) indeed yields a sine and a cosine term (Fig. 3a), which can be used to construct a rotating vector of which the phase can be tracked to reconstruct the target's displacement. Comparing the reconstructed displacement using this vector to the reference measurement obtained by a triangulation sensor shows that both displacement measurements are equal in shape (Fig. 3b). The displacement measured via SMI is approximately 3 μm larger than the displacement obtained by the reference. However, the reference measurement has a resolution of 4.5 μm, so the measurements can be considered to be the same in amplitude. Moreover, the standard deviation of the displacement measurements shows that the SMI method applied is more precise than the reference triangulation sensor used. The time lag between the control signal and the displacements can be considered to be equal too: the difference in time lag of 0.43 ms is 3-4 times smaller than the standard deviation of the timing measurements. Finally, Fig. 3b shows that the SMI displacement measurement may contain a DC value, depending on the time instant at which the measurement has been started during the cycle of the loudspeaker. In the context of PPG motion artifact handling, such a DC component is not useful and can be removed.

The measurements have confirmed that inaccuracies in displacement as a result of imperfect normalization of the vector coordinates, and shot noise, thermal noise and quantization noise are in the order of 10^{-8} m. Theoretically it has been shown that the change in wavelength caused by feedback yields an error in the order of 10^{-8} m. An error of 10^{-8} m is sufficient to accurately measure sensor displacements of $10^{-4} - 10^{-3}$ m. It should be noted that speckle effects have been neglected in this analysis. Though normalization sufficiently suppresses the effect of speckle in the laboratory setup, speckle effects may have to be included in the accuracy analysis when measuring displacement with respect to skin.

V. Conclusion

It has been demonstrated that displacement between a laser diode and a Delrin skin phantom can be accurately measured using the SMI effect of a laser diode of which the driving current is amplitude modulated. Therefore, this method can be applied to measure displacement between a PPG sensor and skin, and used to determine whether sensor displacement correlates to optical motion artifacts in PPGs.

References

[1] H. H. Asada, P. Shaltis, A. Reisner, S. Rhee, and R. C. Hutchinson, "Mobile monitoring with wearable photoplethysmographic biosensors," *IEEE Engineering in Medicine and Biology Magazine*, vol. 22, no. 3, pp. 28–40, May/June 2003.

[2] M. J. Hayes and P. R. Smith, "Artifact reduction in photoplethysmography," *Applied Optics*, vol. 37, no. 31, pp. 7437–7446, November 1998.

[3] M. H. Koelink, M. Slot, F. F. M. de Mul, J. Greve, R. Graaff, A. C. M. Dassel, and J. G. Aarnoudse, "Laser Doppler velocimeter based on the self-mixing effect in a fiber-coupled semiconductor laser: theory," *Applied Optics*, vol. 31, no. 18, pp. 3401–3408, June 1992.

[4] K. Petermann, *Laser diode modulation and noise*, T. Okoshi and T. Kamiya, Eds. Kluwer Academic Publishers, KTK Scientific Publishers, 1988.